Low Temperature Physics/Fizika Nizkikh Temperatur, 2016, v. 42, No. 7, pp. 748–755

Theoretical analysis of the kinetics of low-temperature defect recombination in alkali halide crystals

V.N. Kuzovkov[1], A.I. Popov[1], E.A. Kotomin[1,2], A.M. Moskina[1], E. Vasil'chenko[3], and A. Lushchik[3]

[1]*Institute of Solid State Physics, 8 Kengaraga Str., Riga LV 1063, Latvia*
E-mail: kuzovkov@latnet.lv

[2]*Photochemistry Center, Russian Academy of Sciences Str., Moscow, Russia*

[3]*Institute of Physics, University of Tartu, 1 W. Ostwald Str., Tartu 50411, Estonia*

Received April 25, 2016, published online May 25, 2016

We analyzed carefully the experimental kinetics of the low-temperature diffusion-controlled *F*, *H* center recombination in a series of irradiated alkali halides and extracted the migration energies and pre-exponential parameters for the hole *H* centers. The migration energy for the complementary electronic *F* centers in NaCl was obtained from the colloid formation kinetics observed above room temperature. The obtained parameters were compared with data available from the literature.

PACS: 61.72.Cc Kinetics of defect formation and annealing
61.82.Ms Insulators (radiation effects in ..)
64.70.pv Colloids.

Keywords: alkali halides; defect; diffusion; reaction; ionizing radiation.

1. Introduction

It is generally accepted that radiation instability of the majority of alkali halide crystals (AHCs) is determined by the creation of interstitial-vacancy (*i*–*v*) pairs of Frenkel defects (FDs) in an anion sublattice via the decay of self-trapping excitons or the recombination of conduction band electrons with self-trapped holes (V_k centers), i.e., the so-called excitonic and electron-hole (*e*–*h*) mechanisms of FDs creation (see [1–8] and references therein). About 95% of such anion FDs are short-lived ones (10^{-11}–10^{-1} s) [3–7,9–11], while the accumulation of so-called long-lived structural defects which are stable for hours, days and months plays a crucial role in radiation-induced material degradation, therefore, being a limitation for many applications [12–16]. It is experimentally proved that low-temperature irradiation leads to the creation of two types of FD pairs: a classical Frenkel pair is defined as a positively charged anion vacancy (v_a, α center) and an interstitial halide ion (i_a^-, *I* center), while a pair of neutral FDs consists of an *F* center (an electron trapped by an anion vacancy, $v_a e$) and an *H* center (a dihalide molecule X_2^- located in one anion site, i_a^0) [1–9,17–19].

It is generally accepted that the energy of various radiation-induced electronic excitations (EEs) in AHCs is partly transformed into *F*–*H* pairs, while α–*I* pairs are formed due to the tunnel recharging of primary close *F*–*H* or due to the recharge of *F* and *H* centers into α and *I* with the participation of *e*–*h* pairs. On the other hand, the spectra of stable *F*–*H* and α–*I* pair creation by vacuum ultraviolet (VUV) radiation measured in a number of AHCs using highly sensitive luminescence methods do not totally coincide, and the formation of primary α–*I* under certain conditions is not excluded [2,20–24].

F, *H* as well as α and *I* centers manifest themselves as typical bands of radiation-induced optical absorption (see, e.g., [19]). Interstitials in the form of *H* centers are detectable by the electron paramagnetic resonance (EPR) method that provides direct information about microstructure and surrounding of a paramagnetic center [25–29]. However, both these methods can be used only at rather high concentration of FDs, i.e., after "integral" x-irradiation. On the other hand, the creation of small amount of *F*–*H* and α–*I* pairs

by, VUV radiation that selectively formed various intrinsic EEs in a thin crystal layer was also detected using luminescent methods [20–23,26,30]. The so-called α luminescence, the stimulation spectrum of which coincides with the α absorption band, can be taken as a measure of radiation-induced α centers (α–I pairs), while a typical tunnel luminescence can be considered as a measure of F–H pairs, that undergo radiative recharging under stimulation within the F absorption band. The use of low-dose VUV irradiation allowed to realize the creation regime of isolated FDs pairs, when the average distance between primary F–H pairs considerably exceeds the interdefect distance within FDs pairs [23,26,30].

At liquid helium temperature, radiation-induced stable F–H and α–I pairs consist of immobile defects, while interstitials (at first I centers and then H centers) easily become mobile with the temperature rise up to ~20–40 K and recombine with F centers remaining immobile even highly above room temperature. The thermal annealing of radiation-induced F–H and α–I pairs in AHCs was experimentally investigated in details by means of various versions of thermoactivation spectroscopy. Measuring the intensity (light sum) of typical photostimulated luminescence, several stages of the annealing of F–H or α–I pairs were revealed in VUV-irradiated AHCs. In x-irradiated AHCs, the pulse annealing curves of the EPR signal of the H centers as well as the annealing of typical optical absorption bands of FDs were measured as well. In addition, a number of peaks of thermally stimulated luminescence usually accompanies the thermal annealing.

If the recombination occurs between defects within spatially separated (isolated) pairs, the annealing stages are connected with the migration distance of a mobile defect toward its complementary counterpart in the pair. In x-irradiated AHCs, the situation is more complicated because besides F–H or α–I pairs, complex groups of spatially correlated defects, for instance F–I–V_k triplets, are also formed during irradiation (see, e.g., [2,17,31–33]). The formation of such and similar defect triplets/groups was detected in KBr, NaCl, and LiF even under low-temperature VUV irradiation, when an exciting photon is able to form simultaneously two-three spatially close EEs (via the multiplication process), which undergo transformation into various defect groups [32–34]. Under such irradiation conditions, the certain annealing stages of a certain defect can be connected with the mobility of other defects and their interaction with the partners from a defect group. As a result, a rise stage was detected at the annealing of paramagnetic H centers in x-irradiated KBr and KCl crystals due to a secondary reaction $I + V_k \rightarrow H$ within a F–I–V_k triplet [22,23,25,26].

It is worth noting that the average interdefect distance r_{FH} within F–H pairs depends on the elementary mechanism of their creation and, respectively, a type of irradiation. If the exciting photons form anion excitons, the value of r_{FH} is larger than that for F–H pairs photocreated via e–h recombination. The annealing of F–H pairs is accompanied by several peaks of thermally stimulated luminescence connected with different migration distances (number of jumps) of a mobile H center toward a complementary immobile F center.

By means of highly sensitive luminescent methods, it is possible to select F–H (and α-I) pairs with a certain value of r_{FH}. For instance, tunnel recharging (F–$H \rightarrow \alpha$-I transformation) occurs in F–H pairs with larger values of r_{FH} (by a few interanion distances) under additional F-stimulation–optical excitation of the existing F centers. The relative amount of H centers that undergo such recharging can be determined by direct EPR method [23,25,26].

The microstructure of paramagnetic H centers in five investigated AHCs is rather different. In NaCl, H centers are oriented along <111> crystallographic directions, while in KCl, RbCl, KBr, and RbBr crystals the orientation is along <110>. H center can be only approximately considered as a dihalide molecule X_2^- located in one anion site. There is additional hyperfine interaction of X_2^- with two more neighbor anions along [110], i.e., strictly, an H center is X_4^{3-}. This fact is obtained from the analysis of EPR spectrum (and it's spin-Hamiltonian). The value of such superfine interaction $X^- - X_2^- - X^-$ is high in KBr, RbBr and KCl, but is very weak in RbCl [25]. These circumstances (orientation and superfine interaction) influence the initial separation of F and H centers formed as an F–H pair and, as a result, the thermal stability of these pairs (and especially α-I pairs formed at a subsequent tunnel recharging of F–H).

Concluding, only a detailed complex analysis of the data received by all the above-mentioned versions of thermoactivation spectroscopy allowed to select the annealing stage connected with the recombination of a becoming mobile interstitial with its counterpart from a FDs pair. The purpose of the present paper is to compare the experimental results available in the literature on the recombination of radiation-induced mobile H interstitials with immobile F centers at low temperatures in the series of alkali halides (NaCl, KCl, RbCl, KBr, RbBr) with the quantitative computer simulations of these diffusion-controlled processes. Despite numerous experimental studies of the kinetics of primary defect annealing upon temperature increase, obtained by a number of optical and magnetic methods, very little quantitative information is available on the defect migration energies and their pre-exponential factors. These parameters are necessary for the prediction of the kinetics of possible secondary reactions and, in general, material radiation stability. Previous studies performed on KCl and KBr crystals were focused mostly on spatially correlated defect pairs (F–H and α–I) [11,35–38], while this paper deals with the recombination kinetics of spatially uncorrelated complementary defect pairs.

2. Method

Numerous experimental studies provide data on the changes of radiation defect concentration versus heating (annealing) temperature caused by mobile defect encounter and recombination. Usually, the temperature in these experiments is a linear function of time. As mentioned above, our purpose is to extract the key diffusion parameters — migration energy and pre-exponential factor from the experimental data for alkali halides.

Change of F, H defect concentration in the bimolecular recombination is described by the standard kinetic equation

$$\frac{dn_F(t)}{dt} = -K(t)n_F(t)n_H(t), \qquad (1)$$

where $K(t)$ is the recombination rate.

Assuming equal F and H concentrations $n_F/n_0 = n_H/n_0 = C$ with initial concentration n_0, this reads

$$\frac{dC(t)}{dt} = K(t)n_0C^2(t). \qquad (2)$$

Thus, the defect concentration decay is

$$C(t) = \frac{1}{1 + n_0\int\limits_0^t K(t)dt}, \qquad (3)$$

where the diffusion-controlled reaction rate K is proportional to the mutual diffusion coefficient D [39]

$$K = 4\pi DR \qquad (4)$$

and, thus, depends exponentially on the defect migration energy E_a, $D = D_0\exp(-E_a/kT)$, whereas R is the recombination radius. In our case of F, H defects, E_a is the migration energy of a more mobile defect (an H center). Finally, assuming the temperature increase with the heating rate $\beta(t)$, one gets the following relation for the concentration decay

$$C_i = \frac{1}{1 + 4\pi(n_0D_0R\int\limits_{T_0}^{T_i} e^{-E_a/k_BT}\beta^{-1}(T)dT}. \qquad (5)$$

In most experiments, $\beta(t) = \beta = \text{const}$ and we get two control parameters: the migration energy E_a, and pre-exponential factor

$$X = n_0D_0R/\beta. \qquad (6)$$

We fitted below these two key parameters, E_a and X to the available experimental kinetics by means of the least square method. The typical value of $X \sim 10^8$ K^{-1} could be estimated using the commonly known basic parameters: $n_0 = 10^{17}$ cm^{-3}, $D_0 = 10^{-3}$ cm^2·s^{-1}, $R = 10^{-7}$ cm, the constant heating rate $\beta \sim 0.15$ Ks^{-1}. The estimates of the F, H migration energies in alkali halides available from the literature are summarized in Table 1.

Table 1. Activation energy E_a (in eV) assigned to H center migration

	This work	Other studies	Reference
LiF	–	0.13	40
–	–	0.11	41
–	–	0.138	42
KBr	0.087–0.10	0.090	43
–	–	0.081	44
RbBr	0.065	0.08	45
CsBr	–	0.035	45
KCl	0.12	0.075	43
–	–	0.12–0.13	46
NaCl	0.089	–	–
–	–	0.08	47
–	–	0.09–0.17 (theor)	47
RbCl	0.078	–	–
KI	–	0.075	45

3. Main results

3.1. NaCl

There are several available studies of the H center recombination kinetics in NaCl crystals. The annealing kinetics curves obtained in the temperature range around 35 K using both EPR [26] and optical absorption method [48] are shown in Fig. 1 by symbols, while solid lines present the results of our simulation. The values of the simulated migration energy, $E_a = 0.05$–0.09 eV agree well with those known for the H centers from the literature (see Table 1). Please note several annealing stages in the optical measurements [48]: the first one is caused by the thermal annealing of correlated F, H centers, the second one is due to recombination of uncorrelated defects, and, lastly, the third stage, presented as a small peak at about 40 K, is related to the delocalization of an H center from a metal impurity trap (i.e., thermal destruction of H_A centers). As Fig. 1(b) shows, the fitting curve only partly covers the last stage, reduces the curve slope and, therefore, causes the lowering of the value of the estimated migration energy. The EPR data [26] from Fig. 1(a) are free from this problem (signals from H and H_A centers can be separated) and thus, the estimated value of $E_a = 0.09$ eV looks more reliable. The parameter X is large in both cases, as expected for the regular diffusion in a single crystal.

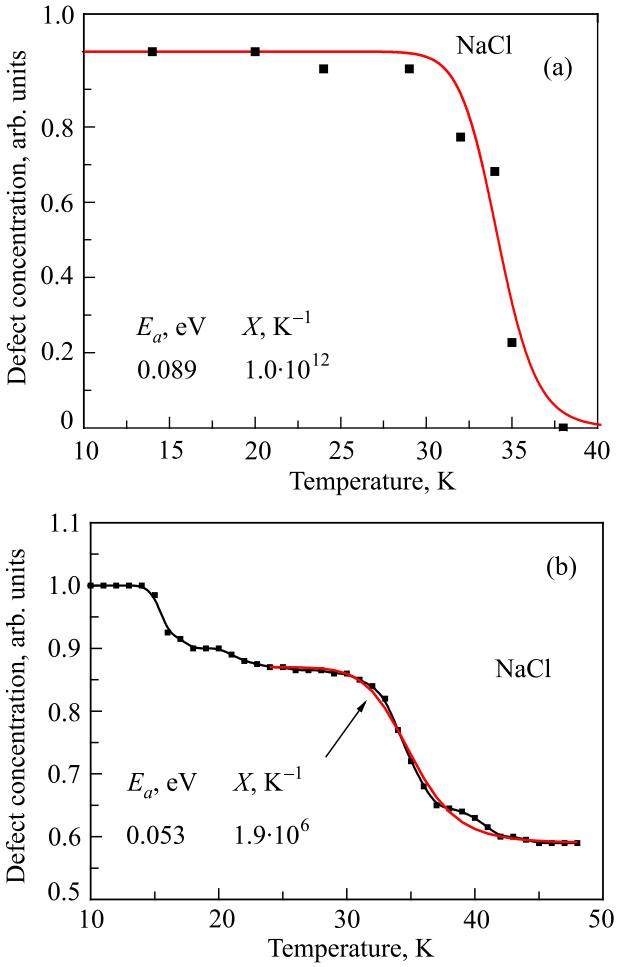

Fig. 1. The annealing kinetics of the H center concentration as measured in a NaCl single crystal by means of the EPR (■, according to Ref. 26) or optical absorption (●, [48]). The solid line is theoretical fitting. The obtained migration energy E_a and pre-exponential factor X are shown in a legend (see text for details).

3.2. KCl

The H center annealing kinetics observed above 45 K (see Fig. 2) is characterized by the slightly higher migration energy of 0.12 eV, as compared to the NaCl case, while the large X factor is qualitatively similar. It is worth noting that a small increase stage at 40–45 K is due to the H center formation because of the α–I pair annealing at lower temperatures. The energy estimate is close to that evaluated by Kolk [46] and considerably larger than that assigned by Ueta [43].

3.3. KBr

The analysis of I center thermal annealing (via recombination of mobile I centers with still immobile α centers) is shown in Fig. 3. The experimental points are taken from Ref. 49, and the simulation (solid line) is performed for the second stage around 15 K — annealing via uncorrelated defect recombination and suggests quite low migration energy of $E_a = 0.026$ eV for the I centers. On the other hand, analysis of the optical absorption annealing for the F, H centers in the same KBr crystal [48] around 40 K (see Fig. 4) yields similar energies for both defect annealing kinetics (0.087 and 0.10 eV) since in both cases just an H center is a mobile recombining partner. These values of E_a are close to previous estimates by other authors (see Table 1). As one can also see, a fraction of F centers survives the recombination since some of mobile H centers undergo trapping by metal impurities with the formation of H_A centers and, thus, avoid their recombination with the F centers. Note that a simple relation for the destruction temperature T_d of the H_A centers as a function of the difference in the radii for a host cation and impurity in KBr and KCl crystals has been presented and theoretically justified in [50].

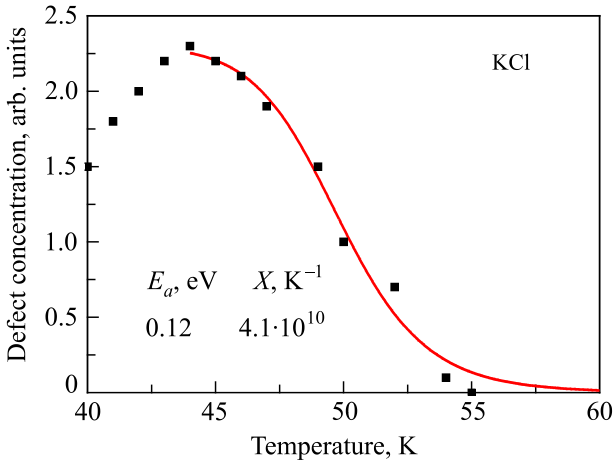

Fig. 2. The annealing kinetics of radiation-induced H centers in KCl measured by the EPR method (■, according to Ref. 26), solid line presents the result of the present simulation.

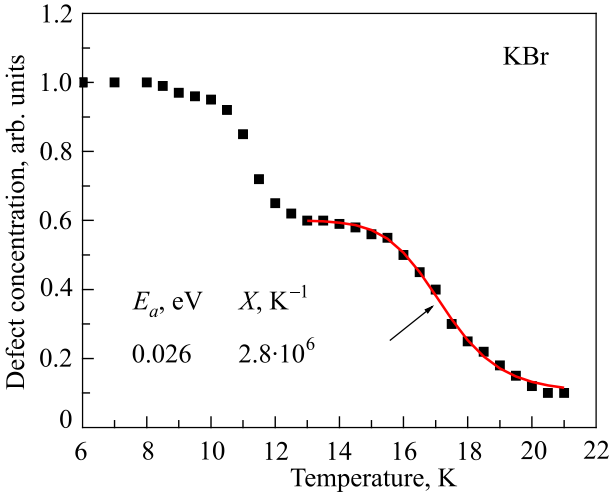

Fig. 3. The annealing kinetics of radiation-induced I centers in a KBr crystal after simulation (solid line) or as measured via the thermal annealing of the optical absorption band according to Ref. 49.

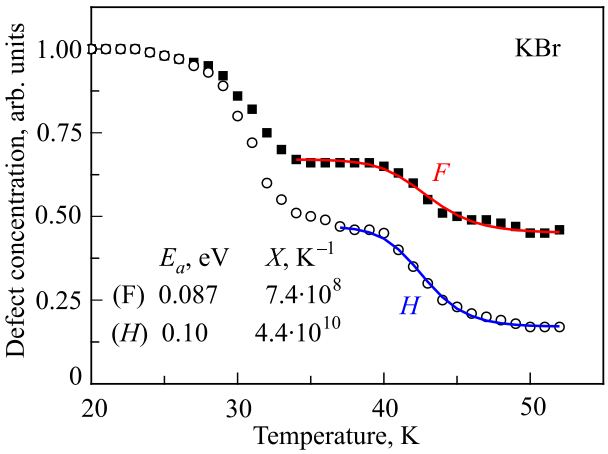

Fig. 4. (Color online) The annealing kinetics of radiation-induced *F*, *H* centers in KBr measured via the thermal annealing of optical absorption bands related to *F* (■) or *H* (○) centers [48]. Solid lines shows the result of present simulation.

3.4. RbCl

The *H* center migration in RbCl [26] (see Fig. 5(a)) is characterized by the energy of 0.078 eV, slightly lower than in two other chlorides, KCl and NaCl. The pre-exponential factor *X* is also smaller. To our knowledge, this is the first estimate for the *H* center migration energy in RbCl.

3.5. RbBr

The *H* center migration energy of 0.065 eV in RbBr (see Fig. 5(b)) derived from the pulse annealing of the EPR signal of *H* centers [26] is lower than that in both KBr and RbCl crystals (see Table 1). It is a reasonable result because the lower *H* center migration energy is, the larger is the overlap of two nearest anions that depends on radii of both cations and anions. The previous estimate of E_a was considerably higher. The pre-exponential factor *X* is also smaller than that in KCl.

3.6. NaCl *at high temperatures*

All the above-discussed low-temperature annealing kinetics allowed us to obtain the migration energies for the *H* centers, which become mobile at temperatures when electronic *F* centers are totally immobile. In order to get information on the *F* center motion, one has to analyze the kinetics caused by the mobile *F* centers. It is known that mobile *F* centers produce more complex defects containing the dimer (*M* centers), trimer (*R*), tetramer (*N*) *F* aggregates and finally, metal colloids [16,51–53]. Such kinetics were studied in the electron-irradiated NaCl crystals in particular [54]. It was shown that the *F* center concentration decay above 400 K is accompanied by a simultaneous growth of the *colloid X* absorption band. In this case, the

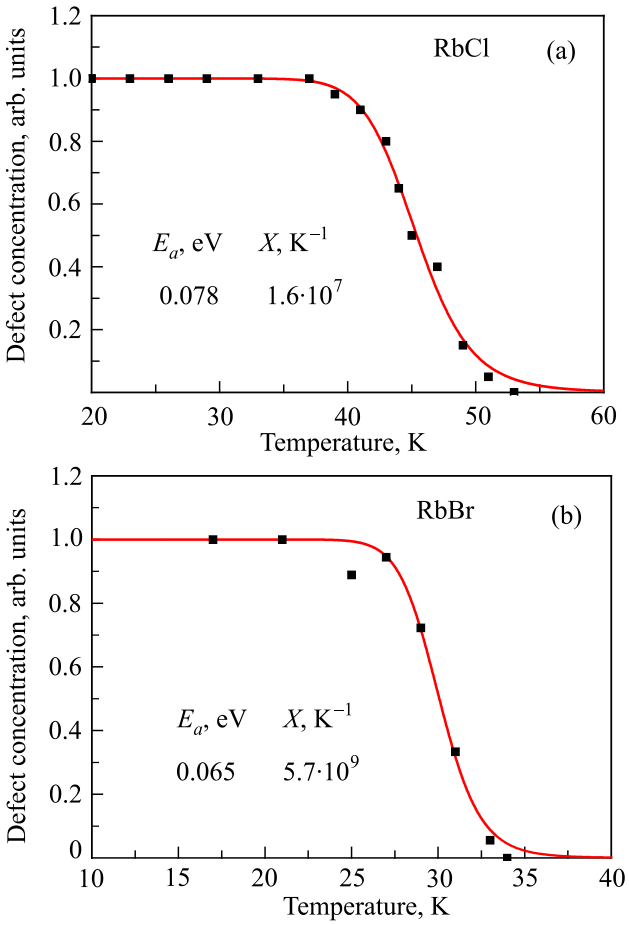

Fig. 5. (Color online) The annealing kinetics of radiation-induced *H* centers in RbCl (a) and RbBr crystals (b) measured by the pulse annealing of the EPR signal [26] or as the result of the present simulation (solid curves).

main mechanism of colloid formation is the mutual encounter of mobile *F* centers and their aggregation caused by an elastic attraction, which can be characterized by the interaction energy ε for the nearest neighbor defects. The relevant theory and computer program were described earlier [52,53,55,56] and successfully applied to the kinetics of colloid formation under intensive electron irradiation of CaF_2 [57] and LiF [58] as well as for thermochemically-reduced MgO and Al_2O_3 [16,52,56,59,60].

Figure 6 depicts the calculated annealing kinetics of *F* centers for different values of E_a and simultaneous temperature-induced growth of the concentration of colloids consisting of different number of defects (N_0) in a NaCl crystal. According to Fig. 6(a), the best agreement with experimental data (given by filled squares according to Ref. 54) is achieved for the *F* migration energy of $E_a = 1.13$ eV which is close to the previous estimates [16]. It is commonly accepted that the peak energy and halfwidth of the *X*-absorption band of metal colloids depend strongly on colloid size: very small colloids possess broad structureless bands, whereas the well-pronounced experimental optical band obtained in Ref. 54 and pre-

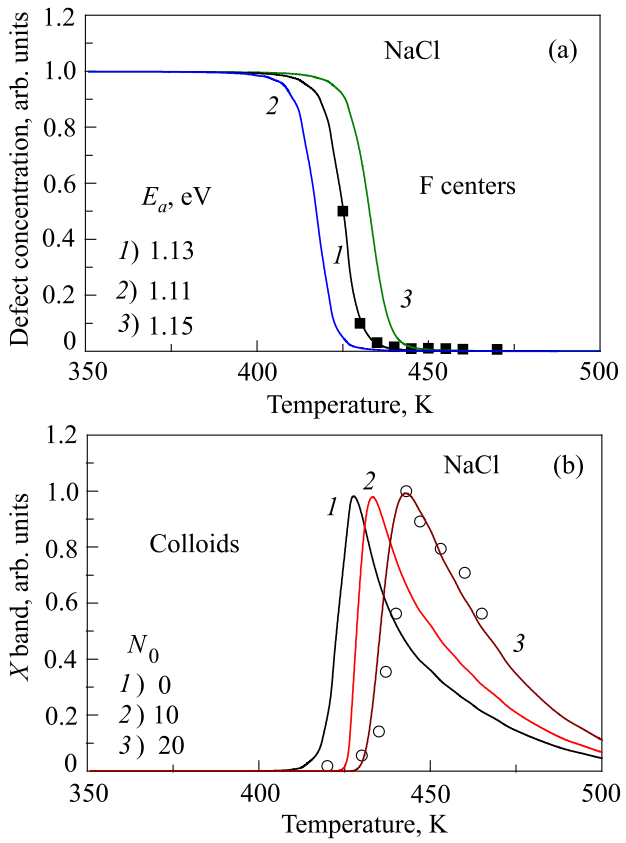

Fig. 6. (Color online) The calculated annealing kinetics (solid lines) of the *F* center concentration for different values of E_a (a) as well as the growth of the colloid concentration with the certain defect number N_0 (b, see text for details) in a NaCl crystal. The experimental points are taken from Ref. 54 and are shown by filled squares and open circles.

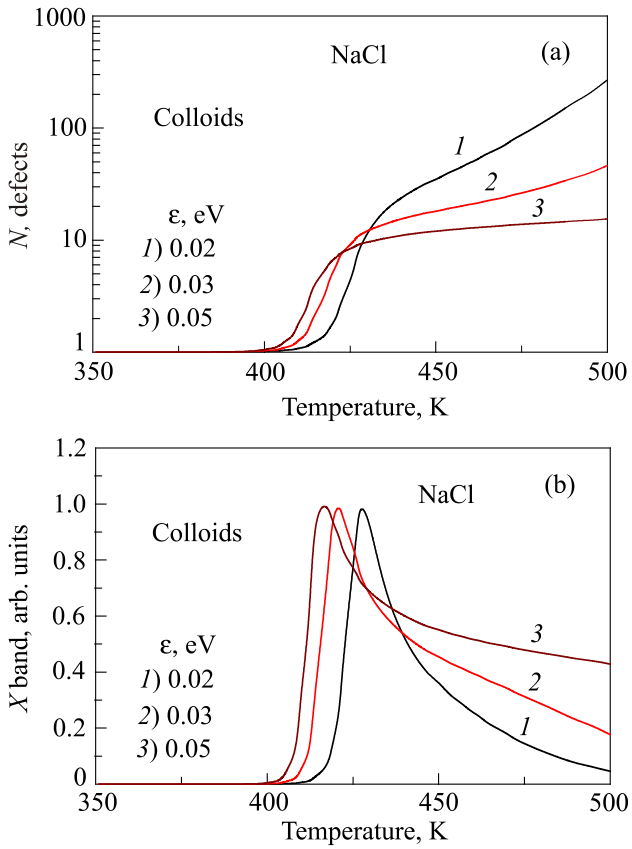

Fig. 7. (Color online) The calculated temperature dependences of the average number of defects within a colloid (a) and of the concentration of colloids with a certain $N_0 = 0$ (b) for different attraction energies ε between *F* centers in a NaCl crystal.

sented in Fig. 6 definitely corresponds to large-size colloids. We assume here the Poisson distribution of colloids in size. Figure 6(b) shows that the best agreement with experimental data is achieved assuming that each colloid contains at least $N_0 = 20$ defects.

Lastly, Fig. 7 demonstrates the influence of the attraction energy between *F* centers ε on the temperature dependence of an average number of defects within a colloid N_0 as well as on the temperature dependence of the concentration of colloids with N_0 =0. The latter dependences manifest a peak shape (see Fig. 7(b)) due to a sharp increase in the number of defects within a colloid at low-temperature side and the prevalence of many-defect-containing colloids on the high temperature side. The latter causes the decrease of the colloid concentration (decrease of *X*-band intensity): many small colloids are transformed into several large colloids, and this process is called as Ostwald ripening [51]. When *F* centers do not attract each other ($\varepsilon = 0$), neither *F* center aggregation nor metal colloid formation occurs. For a weak attraction (curves *1* and *2* in Fig. 7(a)) the number of defects in colloids increases, however, already for $\varepsilon = 0.05$ eV only relatively small colloids are formed ($N \sim 10$). These small colloids are not transformed into larger ones due to a strong defect binding within each colloid.

Thus, practically, the range of the attraction energies corresponding to the experiments is quite narrow, 0.02–0.03 eV. Further calculations of the colloid concentration variation with temperature for these attraction energies (see Fig. 7(b)) clearly demonstrate that only $\varepsilon = 0.02$ eV provides the results close to the experiment, whereas higher values of ε (curves *2* and *3*) give broad peaks as well. Thus, the analysis of the colloid band formation in NaCl allows to obtain the *F* center migration and attraction energies with a quite high accuracy.

4. Conclusions

We have estimated for the first time the migration energies of the *H* centers in a series of alkali halides as well as of the *F* centers in NaCl, which are important parameters for phenomenological analysis of radiation-induced processes in these materials. Note that our estimates are much more precise compared to the previous ones (see Table 1) based on a simple assumption of the first- or second-order reaction. Analysis of the pre-exponential factor *X* charac-

terizing the radiation-induced material disordering will be presented in a separate paper.

We are greatful to Prof. Cheslav Lushchik for valuable and stimulating discussions. A.I. Popov and A. Moskina would like to thank the support of State research program IMIS2, while E. Vasil'chenko and A. Lushchik thank the Estonian Research Council–Institutional Research Fundings IUT02-26.

1. Ch.B. Lushchik, I.K. Vitol, and M.A. Elango, *Usp. Fiz. Nauk* **122**, 223 (1977).
2. Ch.B. Lushchik and A.Ch. Lushchik, *Decay of Electronic Excitations with Defect Formation in Solids*, Nauka, Moscow (1989) [in Russian].
3. N. Itoh, *Adv. Phys*. **31**, 491 (1982).
4. R.T. Williams, K.S. Song, W.L. Faust, and C.H. Leung, *Phys. Rev. B* **33**, 7232 (1986).
5. N. Itoh and K. Tanimura, *Optical Eng*. **28**, 1034 (1989).
6. R.T. Williams and K.S. Song, *J. Phys. Chem. Solids* **51**, 679 (1990).
7. N. Itoh and K. Tanimura, *J. Phys. Chem. Solids* **51**, 717 (1990).
8. A. Lushchik, M. Kirm, Ch. Lushchik, and E. Vasil'chenko, *Nucl. Instr. Meth. B* **166–167**, 529 (2000).
9. Y. Kondo, M. Hirai, and M. Ueta, *J. Phys. Soc. Jpn* **33**, 151 (1972).
10. H. Fujiwara, T. Suzuki, and K. Tanimura, *J. Phys.: Condens. Mater*. **9**, 923 (1997).
11. E. Kotomin, A. Popov, and M. Hirai, *J. Phys. Soc. Jpn* **63**, 2602 (1994).
12. R.Y. Zhu, *Nucl. Instr. Meth. A* **413**, 297 (1998).
13. M. Nikl, *Phys. Status Solidi A* **178**, 595 (2000).
14. K. Saiki, Y. Sato, K. Ando, and A. Koma, *Surface Science* **192**, 1 (1987).
15. E. Feldbach, E. Tõldsepp, M. Kirm, A. Lushchik, K. Mizohata, and J. Räisänen, *Optical Materials* **55**, 164 (2016).
16. E.A. Kotomin and A.I. Popov, *Radiation Effects in Solids* Volume: NATO Science Series (2007), vol. 235, p. 153.
17. D.E. Aboltin, V.J. Grabovskis, A.R. Kangro, Ch.B. Lushchik, A.A. O'Konnel-Bronin, I.K. Vitol, and V.E. Zirap, *Phys. Status Solidi A* **47**, 667 (1978).
18. W. Meise, U. Rogulis, F.K. Koschnik, K.S. Song, and J.M. Spaeth, *J. Phys.: Condens. Mater* **6**, 1801 (1994).
19. J. Craword and M. Slifkin (eds.), *Point Defects in Solids,* Pergamon Press, New York–London (1972).
20. E.A. Vasil'chenko, A.Ch. Lushchik, N.E. Lushchik, Ch.B. Lushchik, Kh.A. Soovik, and M.M. Tajirov, *Fiz. Tverd. Tela* **23**, 481 (1981) [*Sov. Phys. Solid State* **23**, 271 (1981)].
21. Ch. Lushchik, J. Kolk, A. Lushchik, N. Lushchik, M. Tajirov, and E. Vasil'chenko, *Phys. Status Solidi B* **114**, 103 (1982).
22. Ch. Lushchik, J. Kolk, A. Lushchik, and N. Lushchik, *Phys. Status Solidi A* **86**, 219 (1984).
23. A.Ch. Lushchik, N.E. Lushchik, and A.G. Frorip, *Fiz. Tverd. Tela* **26**, 2829 (1984) [*Sov. Phys. Solid State* **26** 1711 (1984)].
24. Ch.B. Lushchik and A.Ch. Lushchik, *Izv. AN SSSR Fiz*. **49**, 1972 (1985) [*Bull. Acad. Sci. USSR, Ser. Phys*. (USA) **49**, 96)].
25. Yu.V. Kolk and A.Ch. Lushchik, *Fiz. Tverd. Tela* **28**, 1432 (1986) [*Sov. Phys. Solid State* **28**, 805 (1986)].
26. A.Ch. Lushchik and A.G. Frorip, *Phys. Status Solidi B* **161**, 525 (1990).
27. D. Schoemaker, *Phys. Rev. B* **3**, 3516 (1971).
28. D. Schoemaker and C. Shirkey, *Phys. Rev. B* **6** 1562 (1972).
29. D. Schoemaker and E.L. Yasaitis, *Phys. Rev. B* **5** 4970 (1972).
30. A. Lushchik and Ch. Lushchik, *Izv. AN SSSR Fiz* **56**, 88 (1992) [*Bull. Russ. Acad. Sci. Phys. (USA)* **56**, 201 (1992)].
31. A. Lushchik, I. Kudryavtseva, Ch. Lushchik, E. Vasil'chenko, M. Kirm, and I. Martinson, *Phys. Rev. B* **52**, 10069 (1995).
32. M. Kirm, A. Lushchik, Ch. Lushchik, I. Martinson, V. Nagirnyi, and E. Vasil'chenko, *J. Phys.: Condens. Mater*. **10**, 3509 (1998).
33. S. Nakonechnyi, T. Kärner, A. Lushchik, Ch. Lushchik, V. Babin, E. Feldbach, I. Kudryavtseva, P. Liblik, L. Pung, and E. Vasil'chenko, *J. Phys: Condens. Mater*. **18**, 379 (2006).
34. A. Lushchik, M. Kirm, I. Kudryavtseva, E. Vasil'chenko, and Ch. Lushchik, *Materials Sci Forum* **239-242**, 581 (1997).
35. E.A. Kotomin, A.I. Popov, and R.I. Eglitis, *J. Phys: Condens. Mater*. **4**, 5901 (1992).
36. A.I. Popov, E.A. Kotomin, and R.I. Eglitis, *Phys. Status Solidi B* **175**, K39 (1993).
37. R.I. Eglitis, A.I. Popov, and E.A. Kotomin, *Phys. Status Solidi B* **190**, 2 (1995).
38. A.I. Popov, E.A. Kotomin, and R.I. Eglitis, *Radiat. Eff. Defect. S.* **134**, 1 (1995).
39. E.A. Kotomin and V.N. Kuzovkov, *Rep. Prog. Phys. 1992* **55**, p. 2079 (1992).
40. N. Seifert, W. Husinsky, and G. Betz, *Phys. Rev. B* **43**, 6723 (1991).
41. P. Durand, Y. Farge, and M. Lambert, *J. Phys. Chem. Solids* **30**, 1353 (1969).
42. M. Yabe, *J. Phys. Soc. Jpn*. **36**, 1383 (1974).
43. M. Ueta, *J. Phys. Soc. Jpn*. **23**, 1265 (1967).
44. Z. Postawa, P. Czuba, A. Poradzisz, and M. Szymonski, *Radiat. Eff. Defect. S.* **109**, 189 (1989).
45. M. Saidoh and N. Itoh, *Phys. Status Solidi B* **72**, 709 (1975).
46. Yu.V. Kolk, *PhD Thesis,* University of Tartu (1984).
47. E.A. Kotomin, V.E. Puchin, and P.W.M. Jacobs, *Philos. Mag. A* **68**, 1359 (1993).
48. K. Tanimura and T. Okada, *Phys. Rev. B* **21**, 1690 (1980).
49. N. Itoh, B.S.H. Royce, and R. Smoluchowski, *Phys Rev*. **137A**, A1010 (1965).
50. A.I. Popov and E.A. Kotomin, *Solid State Commun*. **106**, 289 (1998).
51. A.E. Hughes and S.C. Jain, *Adv. Phys*. **28**, 717 (1979).
52. V.N. Kuzovkov, A.I. Popov, E.A.Kotomin, M.A. Monge, R. Gonzalez, and Y. Chen, *Phys. Rev. B* **64**, 064102 (2001).
53. E.A. Kotomin, V.N. Kuzovkov, and A.I. Popov, *Radiat. Eff. Defect. S.* **155**, 113 (2001).

54. K. Inabe, N.Takeuchi, and S. Owaki, *Nucl. Instr. Meth. B* 91, 201(1994).
55. V.N. Kuzovkov and W. von Nissen, *Phys. Rev. B* **58**, 8454 (1998).
56. E.A. Kotomin, V.N. Kuzovkov, A.I. Popov, M.A. Monge, R. Gonzalez, and Y. Chen, *Nucl. Instr. Meth. B* **191**, 208 (2002).
57. M. Huisinga, N. Bouchaala, R. Bennewitz, E.A. Kotomin, M. Reichling, V.N. Kuzovkov, and W. von Niessen, *Nucl. Instr. Meth. B* **141**, 79 (1998).
58. N. Bouchaala, E.A. Kotomin, V.N. Kuzovkov, and M. Reichling, *Solid State Commun* **108**, 629 (1998).
59. E.A. Kotomin, V.N. Kuzovkov, A.I.Popov, and R.Vila, *Nucl. Instr. Meth. B* **374**, 107 (2016).